Simulation of Tsunami and Flash Floods

S. G. Roberts[1], O. M. Nielsen[2], and J. Jakeman[1]

[1] Department of Mathematics, Australian National University, Canberra, ACT, 0200, Australia [stephen.roberts, john.jakeman]@maths.anu.edu.au
[2] Risk Assessment Methods Project, Geospatial and Earth Monitoring Division, Geoscience Australia, Symonston, ACT, 2609, Australia Ole.Nielsen@ga.gov.au

1 Introduction

Floods are the single greatest cause of death due to natural hazards in Australia, causing almost 40% of the fatalities recorded between 1788 and 2003 [1]. Analysis of buildings damaged between 1900 and 2003 suggests that 93.6% of damage is the result of meteorological hazards, of which almost 25% is directly attributable to flooding [1].

Flooding of coastal communities may result from surges of near-shore waters caused by severe storms. The extent of inundation is critically linked to tidal conditions, bathymetry and topography; as recently exemplified in the United States by Hurricane Katrina. While the scale of the impact from such events is not common, the preferential development of Australian coastal corridors means that storm-surge inundation of even a few hundred metres beyond the shoreline has increased potential to cause significant disruption and loss.

Coastal communities also face the small but real risk of tsunami. Fortunately, catastrophic tsunami of the scale of the 26 December 2004 event are exceedingly rare. However, smaller-scale tsunami are more common and regularly threaten coastal communities around the world. Earthquakes which occur in the Java Trench near Indonesia (e.g. [7]) and along the Puysegur Ridge to the south of New Zealand (e.g. [3]) have potential to generate tsunami that may threaten Australia's northwestern and southeastern coastlines.

Hydrodynamic modelling allows flooding, storm-surge and tsunami hazards to be better understood, their impacts to be anticipated and, with appropriate planning, their effects to be mitigated. Geoscience Australia in collaboration with the Mathematical Sciences Institute, Australian National University, is developing a software application called `ANUGA` to model the hydrodynamics of floods, storm surges and tsunami.

In this paper we will describe the computational model used in `ANUGA`, provide validation of the method using a standard benchmark, and provide

the preliminary results of a tsunami simulation of the coastal region of north eastern Australia, near the city of Cairns.

2 Model

`ANUGA` uses a finite-volume method for solving the shallow water wave equations [8]. The study area is represented by a mesh of triangular cells as in Figure 1 in which water depth h, and horizontal momentum (uh, vh), are determined. The size of the triangles may be varied within the mesh to allow greater resolution in regions of particular interest.

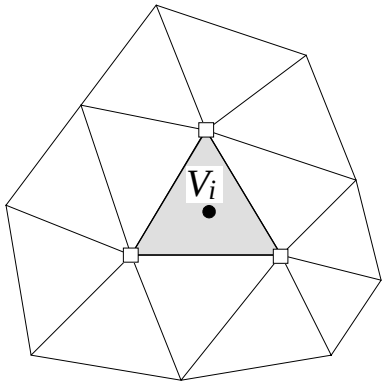

Fig. 1. Triangular elements in the finite volume method.

The shallow water wave equations are a system of differential conservation equations of the form

$$\frac{\partial U}{\partial t} + \frac{\partial E}{\partial x} + \frac{\partial G}{\partial y} = S$$

where $U = \begin{bmatrix} h & uh & vh \end{bmatrix}^T$ is the vector of conserved quantities; water depth h, x momentum uh and y momentum vh. Other quantities entering the system are bed elevation z and stage (absolute water level) w, where the relation $w = z + h$ holds true at all times. The fluxes in the x and y directions, E and G are given by

$$E = \begin{bmatrix} uh \\ u^2h + gh^2/2 \\ uvh \end{bmatrix} \text{ and } G = \begin{bmatrix} vh \\ vuh \\ v^2h + gh^2/2 \end{bmatrix}$$

and the source term (which includes gravity and friction) is given by

$$S = \begin{bmatrix} 0 \\ gh(S_{0x} - S_{fx}) \\ gh(S_{0y} - S_{fy}) \end{bmatrix}$$

where S_0 is the bed slope and S_f is the bed friction. The friction term is modelled using Manning's resistance law

$$S_{fx} = \frac{u\eta^2\sqrt{u^2+v^2}}{h^{4/3}} \text{ and } S_{fy} = \frac{v\eta^2\sqrt{u^2+v^2}}{h^{4/3}}$$

in which η is the Manning resistance coefficient.

The equations constituting the finite-volume method are obtained by integrating the differential conservation equations over each cell of the mesh. By applying the divergence theorem we obtain for each cell an equation which describes the rate of change of the average of the conserved quantities within each cell, in terms of the fluxes across the edges of the cells and the effect of the source terms. In particular, rate equations associated with each cell have the form

$$A_i \frac{dU_i}{dt} + \sum_j (F_{ij} n_{ij1} + G_{ij} n_{ij2}) l_{ij} = A_i S_i$$

where the subscript i refers to the ith cell, A_i is the associated cell area, U_i the vector of averaged conserved quantities, and S_i is the source term associated with each cell. The subscript ij refers to the jth neighbour of the ith cell ($j = 0, 1, 2$), i.e. it corresponds to the 3 edges of the ith cell. We use $F_{ij} n_{ij1} + G_{ij} n_{ij2}$ to denote the approximation of the outward normal flux of material across the ijth edge, and use l_{ij} to denote the length of the ijth edge.

From the average values of the conserved quantities in each of the cells, we use a second order reconstruction to produce a representation of the conserved quantities as a piece-wise linear (vector) function of x and y. This function is allowed to be discontinuous across the edges of the cells, but the slope of this function is limited to avoid artificially introduced oscillations. Across each edge, the reconstructed function is generally discontinuous. The Godunov method (see a good desciption in [6]) usually involves approximating the flux across an edge by exactly solving the corresponding one dimensional Riemann problem normal to the edge. We use the central-upwind scheme of [2] to calculate an approximation of the flux across each edge.

In the computations presented in this paper we use an explicit Euler time stepping method with variable timestepping adapted to the observed CFL condition.

The model output consists of values for w, uh and vh at every mesh vertex at every time step.

3 Software

The components of ANUGA are written in the object-oriented language of Python , with the exception of computationally intensive routines, which are written in the more efficient language of C and deal directly with Python numerical structures. VPython is used to interactively visualise the computational domain and the evolution of the model over time. The output of ANUGA is also being visualised through a netcdf viewer based on OpenSceneGraph which has been written as part of ANUGA. Figures in this paper have been produced using this viewer.

4 Validation

The process of validating the ANUGA application is in its early stages, however initial indications are encouraging.

As part of the Third International Workshop on Long-wave Runup Models in 2004 (http://www.cee.cornell.edu/longwave), four benchmark problems were specified to allow the comparison of numerical, analytical and physical models with laboratory and field data. One of these problems describes a wave tank simulation of the 1993 Okushiri Island tsunami off Hokkaido, Japan [4]. A significant feature of this tsunami was a maximum run-up of 32 m observed at the head of the Monai Valley. This run-up was not uniform along the coast and is thought to have resulted from a particular topographic effect. Among other features, simulations of the Hokkaido tsunami should capture this run-up phenomenon.

The wave tank simulation of the Hokkaido tsunami was used as the first scenario for validating ANUGA. The dataset provided bathymetry and topography along with initial water depth and the wave specifications. The dataset also contained water depth time series from three wave gauges situated offshore from the simulated inundation area.

Figure 2 compares the observed wave tank and modelled ANUGA water depth (stage height) at one of the gauges. The plots show good agreement between the two time series, with ANUGA closely modelling the initial draw down, the wave shoulder and the subsequent reflections. The discrepancy between modelled and simulated data in the first 10 seconds is due to the initial condition in the physical tank not being uniformly zero. Similarly good comparisons are evident with data from the other two gauges. Additionally, ANUGA replicates exceptionally well the 32 m Monai Valley run-up, and demonstrates its occurrence to be due to the interaction of the tsunami wave with two juxtaposed valleys above the coastline. The run-up is depicted in Figure 3.

This successful replication of the tsunami wave tank simulation on a complex 3D beach is a positive first step in validating the ANUGA modelling capability. Subsequent validation will be conducted as additional datasets become available.

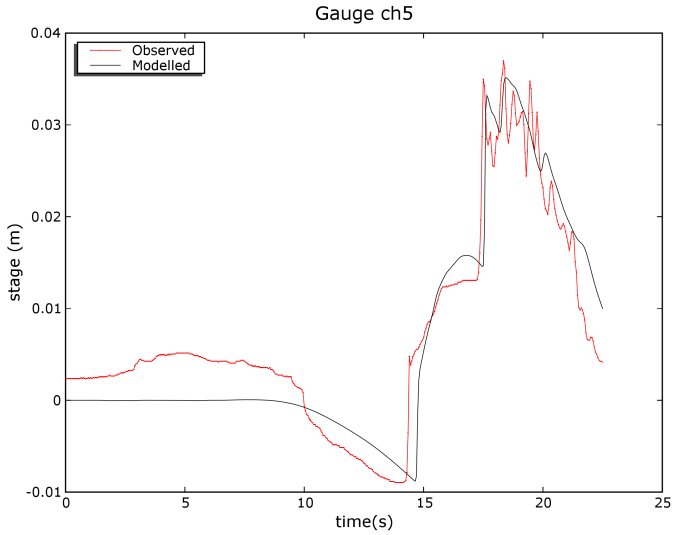

Fig. 2. Comparison of wave tank and ANUGAwater stages at gauge 5.

Fig. 3. Complex reflection patterns and run-up into Monai Valley simulated by ANUGA and visualised using our netcdf OSG viewer.

5 Case Study: Modelling Tsunamis with ANUGA

The Great Barrier Reef is an icon of the north eastern Australian coast line. It is over 2,000 km long, stretching from Cape York to Gladstone off the Queensland coast, and consists of around 3,000 reefs and islands. The hydrodynamic module of ANUGA was used to estimate the impact of these geological formations on an incoming tsunami.

The Tonga-Kermadec subduction zone poses a potential threat to Australia's north-east coastline. A coseismic displacement in the subduction zone could displace billions of tonnes of water that would initiate a tsunami that threatened to destroy Cairns and the surrounding towns and communities. The following details the processes and outcomes of modelling such a tsunami using ANUGA.

To set up a particular scenario using the hydrodynamic module of ANUGA the user must first specify the bathymetry and topography, the initial water stage, boundary conditions such as tidal fluctuations, and any forcing terms such as atmospheric pressure or wind stress. ANUGA contains a mesh generator which allows the user to construct the problem domain and to identify boundaries and special regions. Within these regions the resolution of the mesh can be coarsened or refined and attributes such as stage or elevation redefined to simulate seafloor displacement or submarine mass failure.

In this study a tsunami was modelled on a small region close to Cairn in Northern Australia, between 145 degrees and 25 minutes East and 147 degrees East and between 16 degrees 30 minutes South and 17 degrees 30 minutes South.

In our scenario, stage and friction were set to zero and elevation was taken from a file containing x and y coordinates in Eastings and Northings and an associated altitude. These points were obtained from bathymetry and topography data provided by Geoscience Australia's "2005 Australian bathymetry and Topography grid" and converted into Eastings and Northings. The elevation of the computational domain just described is displayed in Figure 4. Note that the reef bathymetry was not explicitly set, but rather included as part of the Geoscience bathymetry data set used.

All boundaries were defined to be reflective with the exception of the eastern boundary, through which the tsunami would travel. This boundary allows the stage along the border to be set according to some arbitrary function. In the scenario being described the stage was set to be 6 metres at the boundary between 60 seconds and 660 seconds of the simulation and zero at al other times. This is hoped to approximate a possible tsunami generated in the Tonga-Kermadec subduction zone. At this point ANUGA relies on dedicated tsunamigenic models (such as MOST, [5]) to provide the tsunami events resulting from earthquakes at the boundary.

Figure 5 illustrates the evolution of the model tsunami described as it propagates over a small section of the Great Barrier reef adjacent to Cairns. A rainbow scale is used in which red represents the largest negative stage,

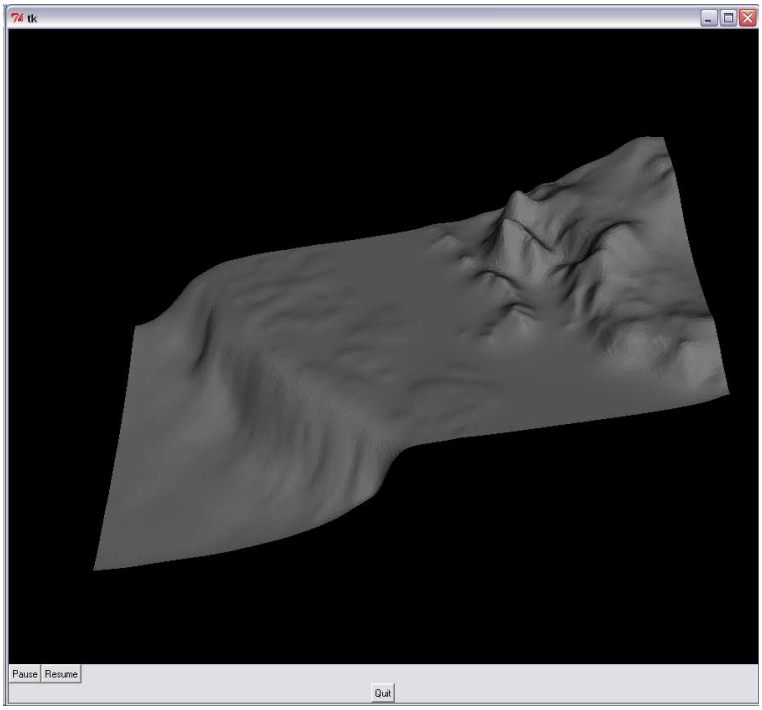

Fig. 4. Elevation of the computational domain. The vertical scale has been exaggerated to extenuate the features on the continental shelf.

yellow the next largest through to green which corresponds to a stage value of zero and then up to blue which represents the largest positive stage values. The colour map was set to display from -10 to 10 metres with stage values outside this range clipped to the maximum and minimum values.

Plots of the domain are shown for times $t = 400$, 800, 1300, 1800, 2300, 2800, 3200 and 3600 s. The plots of the tsunami at $t = 400$ s and $t = 800$ s illustrate the tsunamis decrease in speed and increase in height as it enters shallower water. The plot of the tsunami at $t = 1300$ s displays an interesting feature. A depression in the ocean surface has formed behind the tsunami as it encounters the continental shelf. At $t = 1800$ s a depression of varying depth and extent is present behind the entire length of the tsunami.

At $t = 2300$ s the tsunami has passed over the reef. It appears as though the reef has reduced the height of the tsunami in various regions. The light blue colouring indicates these areas. This behaviour was not evident when the previous colour scheme was used. At $t = 2800$ s inundation of the Cairns coastline has occurred. But again some runup is occurring in advance of the oncoming wavefront. At $t = 3200$ s severe inundation has occurred along the entire southern coast.

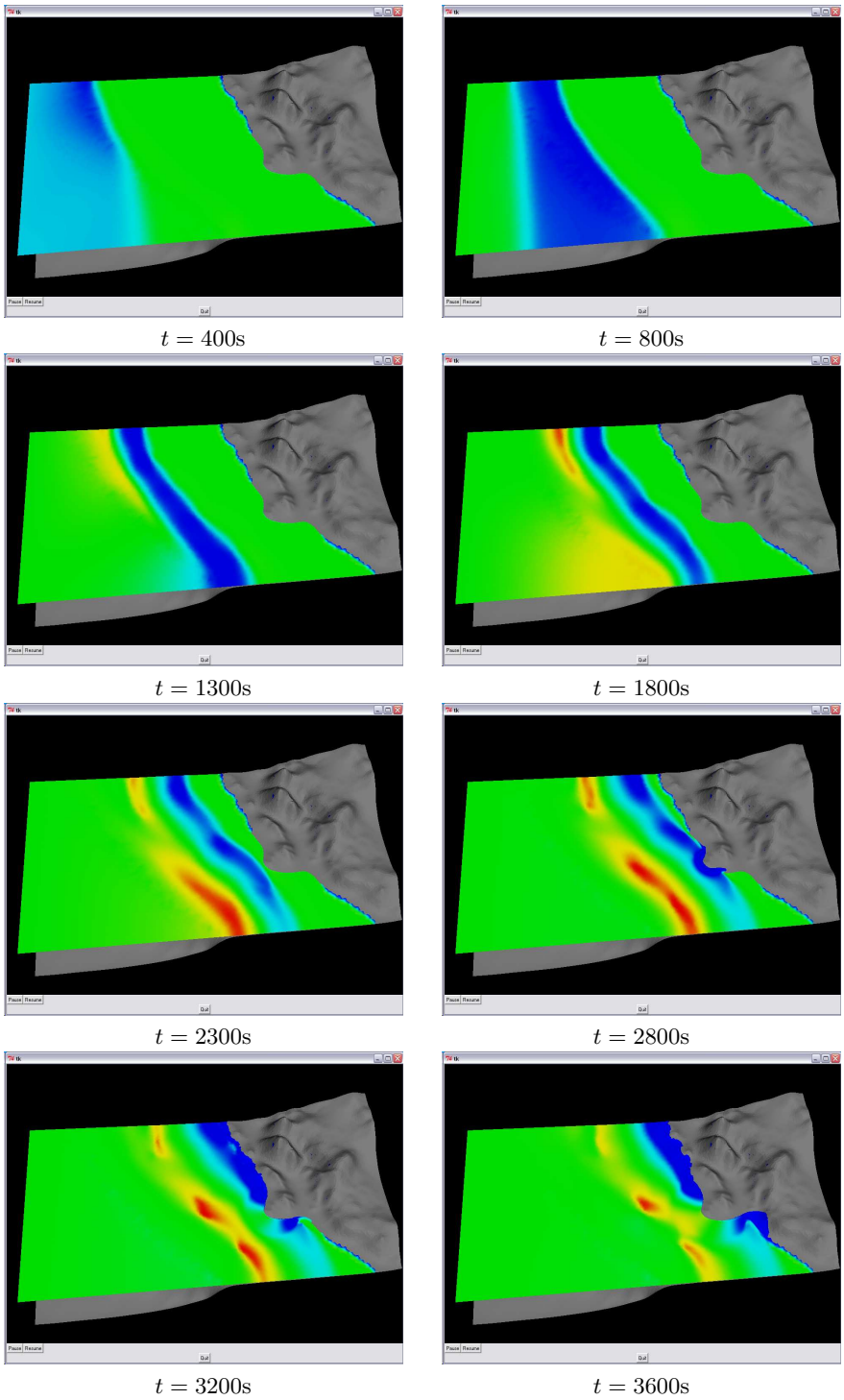

Fig. 5. The evolution in time of a tsunami, initially 6m above the ocean at the Eastern boundary, over the Great Barrier Reef. Note the orientation of the plots is upside down. The southernmost point of the grid is at the top of the picture

The ANUGA model works well for detailed inundation modelling of small sections like those mentioned above but currently less well for synoptic scenarios. To capture e.g. the source modelling and propagation across large regions we use deep water tsunami models such as MOST [5] to provide boundary conditions for AnuGA. In fact, Geoscience Australia has embarked on a program using this approach to predict which coastlines are most at risk taking into account the return period of submarine earthquakes, tsunami wave propagation and the non-linear effects of local bathymetries.

6 Conclusions

ANUGA is a flexible and robust modelling system that simulates hydrodynamics by solving the shallow water wave equation in a triangular mesh. It can model the process of wetting and drying as water enters and leaves an area and is capable of capturing hydraulic shocks due to the ability of the finite-volume method to accommodate discontinuities in the solution.

ANUGA can take as input bathymetric and topographic datasets and simulate the behaviour of riverine flooding, storm surge and tsunami. Initial validation using wave tank data supports AnuGA's ability to model complex scenarios. Further validation will be pursued as additional datasets become available.

ANUGA is already being used to model the behaviour of hydrodynamic natural hazards. This modelling capability is part of Geoscience Australia's ongoing research effort to model and understand the potential impact from natural hazards in order to reduce their impact on Australian communities.

7 Acknowledgements

The authors are grateful to Belinda Barnes, National Centre for Epidemiology and Population Health, Australian National University, and Matt Hayne and Augusto Sanabria, Risk Research Group, Geoscience Australia, for helpful reviews of a previous version of this paper. Author Nielsen publish with the permission of the CEO, Geoscience Australia.

References

1. R. Blong. Natural hazards risk assessment: an australian perspective. Issues in risk science series, Benfield Hazard Research Centre, London, 2005.
2. A. Kurganov, S. Noelle, and G. Petrova. Semidiscrete central-upwind schemes for hyperbolic conservation laws and hamilton-jacobi equations. *SIAM Journal of Scientific Computing*, 23(3):707–740, 2001.

3. J.F. Lebrun, G.D. Karner, and J.Y. Collot. Fracture zone subduction and reactivation across the puysegur ridge/trench system, southern new zealand. *Journal of Geophysical Research*, 103:7293–7313, 1998.
4. M. Matsuyama and H. Tanaka. An experimental study of the highest run-up height in the 1993 hokkaido nansei-oki earthquake tsunami. In *National Tsunami Hazard Mitigation Program Review and International Tsunami Symposium (ITS)*, pages 879–889. U.S. National Tsunami Hazard Mitigation Program, 2001.
5. V. V. Titov and F. I. Gonzalez. Imple-mentation and testing of the method of splitting tsunami (most) model. Technical Memorandum ERL PMEL-112, NOAA, 1997.
6. E. F. Toro. Riemann problems and the waf method for solving the two-dimensional shallow water equations. *Philosophical Transactions of the Royal Society, Series A*, 338:43–68, 1992.
7. Y. Tsuji, S. Matsutomi, F. Imamura, and C.E. Synolakis. Field survey of the east java earthquake and tsunami. *Pure and Applied Geophysics*, 144(3/4):839–855, 1995.
8. C. Zoppou and S. Roberts. Catastrophic Collapse of Water Supply Reservoirs in Urban Areas. *ASCE J. Hydraulic Engineering*, 125(7):686–695, 1999.